

Supporting Information

Low Ceiling Temperature Polymer Microcapsules with Hydrophobic Payloads via Rapid Emulsion-Solvent Evaporation

*Shijia Tang,^{†,‡,⊥} Mostafa Yourdkhani,^{†,⊥} Catherine M. Possanza Casey,^{†,||} Nancy R. Sottos,^{†,‡}
Scott R. White^{*,†,#} Jeffrey S. Moore^{*,†,‡,||}*

[†]Beckman Institute for Advanced Science and Technology, [‡]Department of Materials Science and Engineering, [#]Department of Aerospace Engineering, and ^{||}Department of Chemistry, University of Illinois at Urbana–Champaign, Urbana, Illinois 61801, United States

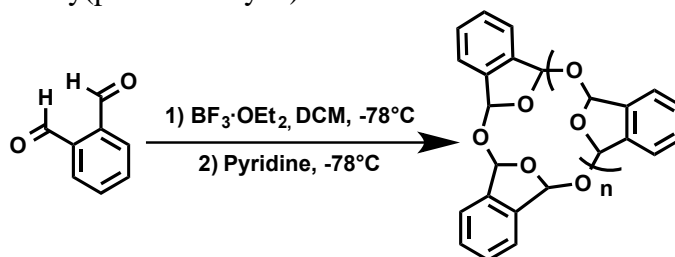
** Corresponding Author*

Email: jsmoore@illinois.edu or swhite@illinois.edu

| | |
|--|------|
| I. Polymer Preparation | S-2 |
| II. Microcapsule Characterization and Parameter Optimization | S-4 |
| II. Triggered Release Experiments | S-14 |
| IV. Microcapsules Prepared with Different Core Materials and Shell Wall | S-14 |

I. Polymer Preparation

(1) Synthesis of Cyclic Poly(phthalaldehyde)

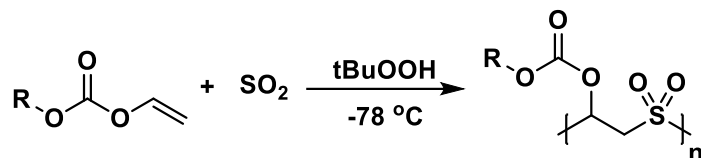


Cyclic poly(phthalaldehyde) (cPPA) was synthesized following literature procedure with slight modification.¹ Generally, 6g purified o-PA was weighed into a Schlenk flask, and the solid was vacuumed and purged under N_2 three times before dissolving in anhydrous dichloromethane (DCM). The solution was cooled to -78°C and boron trifluoride etherate ($\text{BF}_3 \cdot \text{OEt}_2$) was added dropwise. The solution was stirred for 40 min, then 0.2 mL pyridine was added, and the solution was left stirring for another 2 h. The obtained polymer solution was then poured into cold methanol and the polymer was precipitated as a white powder. The polymer was further purified by re-dissolving in DCM and re-precipitating in cooled methanol twice more. The polymer was dried under high vacuum for 24 h and then stored at -20°C . Characterization of the polymer was consistent with the previously reported literature.¹

Table S1. Characterization of Cyclic Poly(phthalaldehyde)

| Polymer | Yield (%) | M_n (kDa) | PDI |
|---------|-----------|-------------|-----|
| cPPA | 78 | 55 | 1.6 |

(2) Synthesis of Poly(olefin sulfone)s



The vinyl butyl carbonate monomers and poly(vinyl butyl carbonate sulfone)s were synthesized following the previously reported literature.² In brief, the polymerizations were as follows: a three-neck round-bottom flask was fitted with a cold-finger, a stir bar, a gas inlet adapter, and a rubber septum. The carbonate monomer (1 g) was added to the flask which was cooled in an acetone/dry ice bath. Sulfur dioxide (40 equiv.) was condensed in a three neck graduated cylinder and subsequently transferred to the three-neck flask via the cold finger. The solution was equilibrated at $-78\text{ }^\circ\text{C}$ for 5 min and then *tert*-butyl hydroperoxide (2.5 mol. %) was added. The polymerization was allowed to proceed for 3 h. The polymer was drawn from the reaction mixture and transferred into cold methanol. After the methanol was decanted, the solid polymer was dissolved in chloroform and re-precipitated in cold methanol. The poly (*tert*-butyl carbonate sulfone) (PV*t*BCS) was dried for 3 h under high vacuum and freeze dried for 6 h to prevent loss of molecular weight at room temperature. The polymers were then stored at $-20\text{ }^\circ\text{C}$. Characterization of the polymers was consistent with the previously reported literature.²

Table S2. Characterization of Poly(olefin sulfone)s

| Polymer | Yield | M_n | PDI |
|-----------------|--------------|----------------------|------------|
| | (%) | (kDa) | |
| PV <i>t</i> BCS | 79 | 19 | 3.2 |

II. Microcapsule Characterization and Parameter Optimization

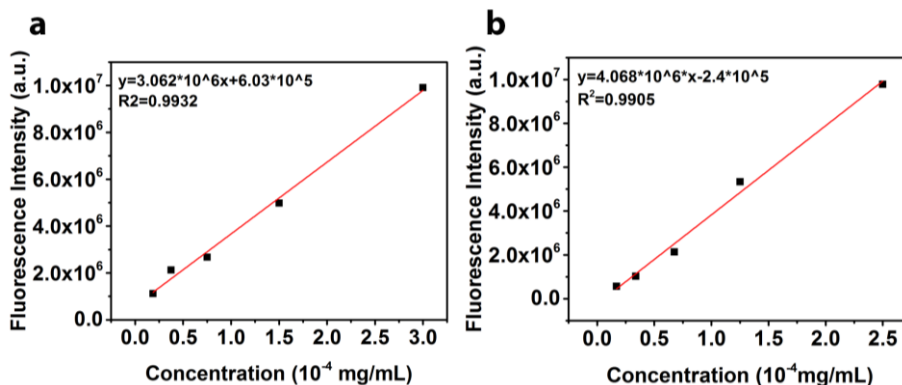


Figure S1. Nile red calibration curve in (a) DCM and (b) heptane.

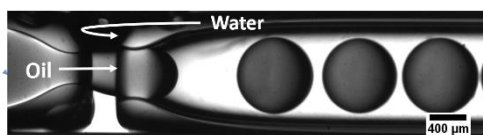


Figure S2. A optical microscopy image of o/w droplets generated by microfluidic device.

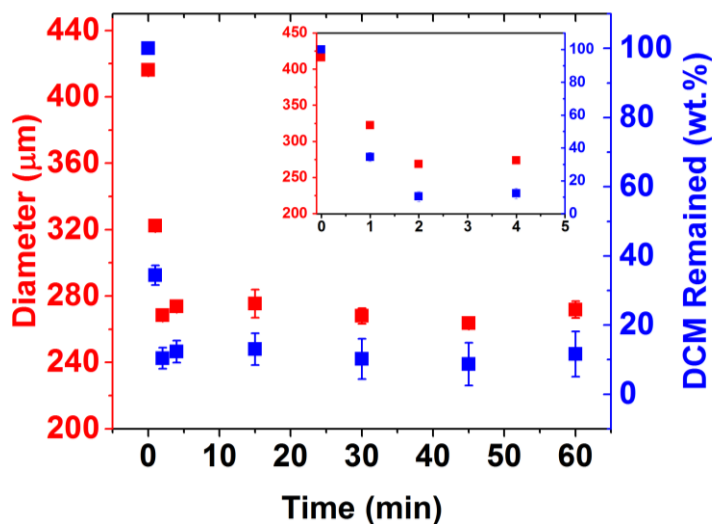


Figure S3. Change in O/W droplet diameter as a function of time during DCM evaporation (red). The DCM remains (blue) is calculated based on the volume change of droplets. Note: The volume change is assumed to be only attributed from DCM evaporation.

Table S3. Summary of Encapsulation Parameters in Microfluidics Emulsification

| Entry | $m_{cPPA}/m_{JJB}/m_{DCM}$ | m_{cPPA}/m_{JJB} | $m_{cPPA} / m_{oil\ phase}^a$ | Evap. ^b | Morphology | ξ (%) ^c |
|-------|----------------------------|--------------------|-------------------------------|--------------------|-------------------------|------------------------|
| M1 | 1.33/1/13.26 | 1.33 | 0.085 | Vac | Core-shell | 107.6 |
| M2 | 1.33/1/17.52 | 1.33 | 0.067 | Vac | Core-shell | 113.5 |
| M3 | 1.33/1.33/13.26 | 1.00 | 0.084 | Vac | Core-shell | 109.4 |
| M4 | 1/1/13.26 | 1.00 | 0.066 | Vac | Core-shell | 100 |
| M5 | 0.66/0.66/13.26 | 1.00 | 0.045 | Vac | Core-shell | 105.6 |
| M6 | 0.33/0.33/13.26 | 1.00 | 0.024 | Vac | Core-shell ^c | - |
| M7 | 0.13/0.13/13.26 | 1.00 | 0.010 | Vac | Core-shell ^c | - |
| M8 | 1/1.14/13.26 | 0.88 | 0.065 | Vac | Acorn | - |
| M9 | 1/2.27/13.26 | 0.44 | 0.060 | Vac | Fail ^d | - |
| M10 | 1/5.77/13.26 | 0.17 | 0.050 | Vac | Fail ^d | - |
| M11 | 1/1.33/13.26 | 0.75 | 0.064 | Vac | Acorn | 30.1 |
| M12 | 1/1/13.26 | 1.00 | 0.066 | S. P. | Acorn | 12.4 |

^a $m_{oil\ phase}=m_{cPPA}+m_{JJB}+m_{DCM}$

^b Vac represents rapid evaporation under reduced pressure; S. P. represents slow evaporation under ambient pressure

^c These microcapsules exhibit microcracks on the shell wall surface

^d No capsules obtained

^e Loading efficiency

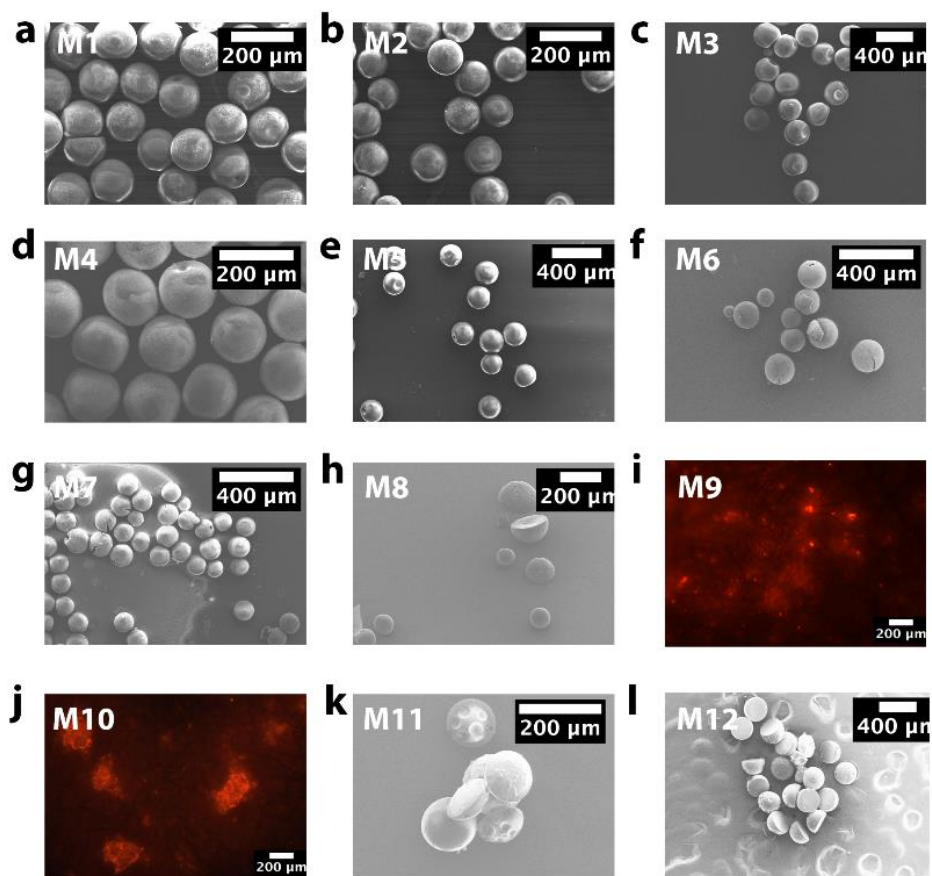


Figure S4. SEM and Fluorescence images of encapsulation products. (a)-(h) and (k)-(l) are SEM images of encapsulation products using composition ratios of entries M1-M8 and M11-12 in Table S3. (i), (j) are fluorescence images of encapsulation products using composition ratios of entry M9 and M10, where no products were recovered from filter paper.

Table S4. Summary of Encapsulation Parameters Used in Bulk Emulsification

| Entry | m_{cPPA}/m_{JJB}/m_{DCM} | m_{cPPA}/m_{JJB} | m_{cPPA} /m_{oil phase}^a | Evap.^b | Morphology | ξ (%)^c |
|--------------|---|---|--|--------------------------|-------------------|--------------------------|
| B1 | 1/0.75/13.26 | 1.33 | 0.067 | Vac | Core-shell | 89.0 |
| B2 | 0.66/0.5/13.26 | 1.32 | 0.046 | Vac | Core-shell | 81.9 |
| B3 | 0.33/0.25/13.26 | 1.32 | 0.024 | Vac | Core-shell | 90.0 |
| B4 | 0.13/0.1/13.26 | 1.30 | 0.010 | Vac | Acorn | - |
| B5 | 1/1/13.26 | 1.00 | 0.066 | Vac | Core-shell | 73.6 |
| B6 | 0.66/0.66/13.26 | 1.00 | 0.045 | Vac | Core-shell | 92.6 |
| B7 | 0.33/0.33/13.26 | 1.00 | 0.024 | Vac | Acorn | - |
| B8 | 0.13/0.13/13.26 | 1.00 | 0.010 | Vac | Acorn | - |
| B9 | 1/1.33/13.26 | 0.75 | 0.064 | Vac | Acorn | 25.2 |
| B10 | 0.66/0.88/13.26 | 0.75 | 0.045 | Vac | Acorn | 34.5 |
| B11 | 1/1/13.26 | 1.00 | 0.066 | S. P. | Acorn | 27.2 |

^a m_{oil phase}=m_{cPPA}+m_{JJB}+m_{DCM}

^b Vac represents rapid evaporation under reduced pressure; S. P. represents slow evaporation under ambient pressure

^c Loading efficiency

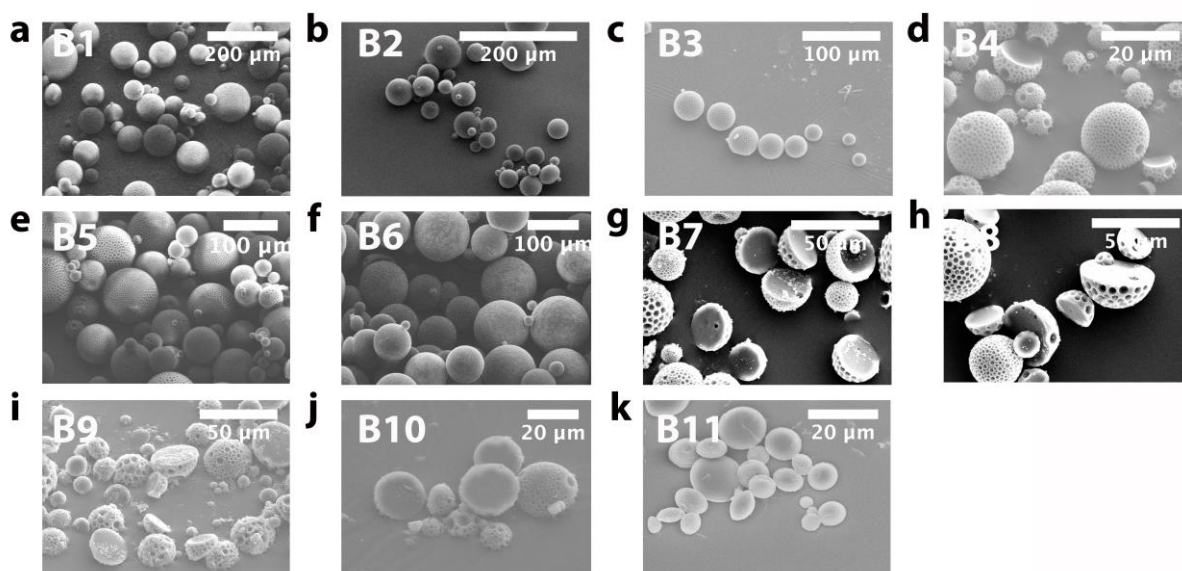


Figure S5. SEM images of cPPA microcapsules fabricated from bulk emulsification. Preparation ratios were following entries B1-B11 listed in Table S4.

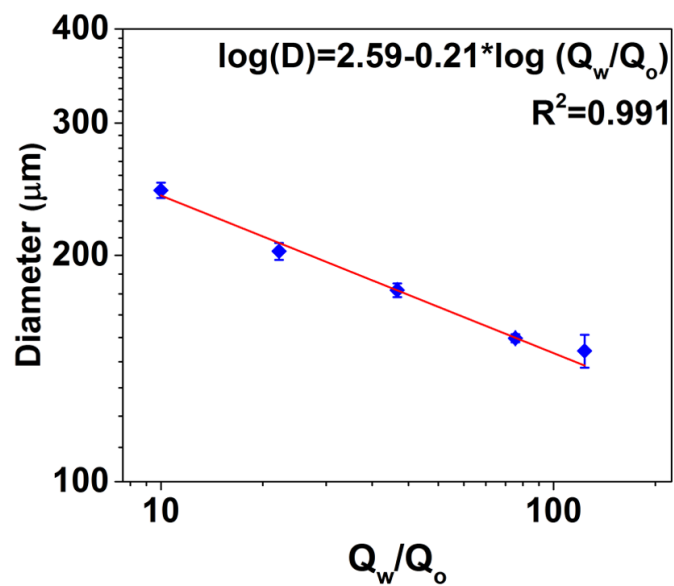


Figure S6. Effect of the ratio of water to oil flow rate (Q_w/Q_o) on microcapsule diameter. A linear relationship (red line) $\log(D)=2.59-0.21 \cdot \log(Q_w/Q_o)$ ($R^2=0.991$) was observed between the logarithmic values of diameter (D) and Q_w/Q_o .

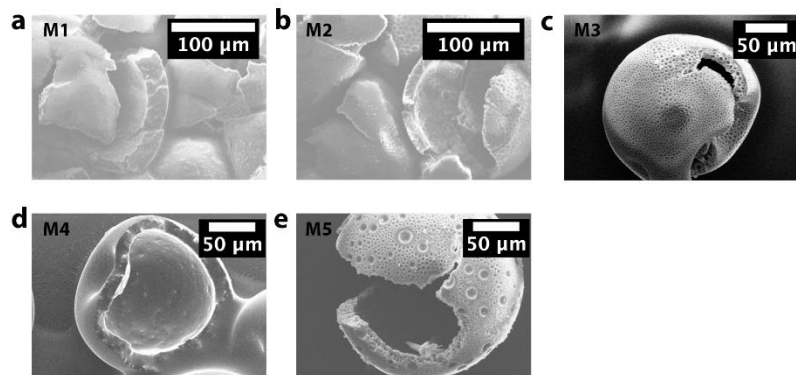


Figure S7. SEM images of crushed cPPA microcapsules showing shell wall thickness for (a) entry M1, (b) entry M2, (c) entry M3, (d) entry M4, and (e) entry M5 listed in Table S3.

Table S5. Summary of Microcapsule Diameter and Shell Wall Thickness

| Entry | Diameter (μm) | Shell Wall Thickness (μm) | Thickness/Diameter Ratio |
|-------|-------------------------------|---|-----------------------------|
| M1 | 139.7 \pm 5.8 | 18.7 \pm 4.1 | 0.133 |
| M2 | 119.9 \pm 4.7 | 12.4 \pm 1.9 | 0.103 |
| M3 | 186.3 \pm 8.9 | 15.7 \pm 1.6 | 0.084 |
| M4 | 168.2 \pm 16.6 | 13.7 \pm 1.7 | 0.081 |
| M5 | 183.7 \pm 5.8 | 16.0 \pm 1.5 | 0.087 |

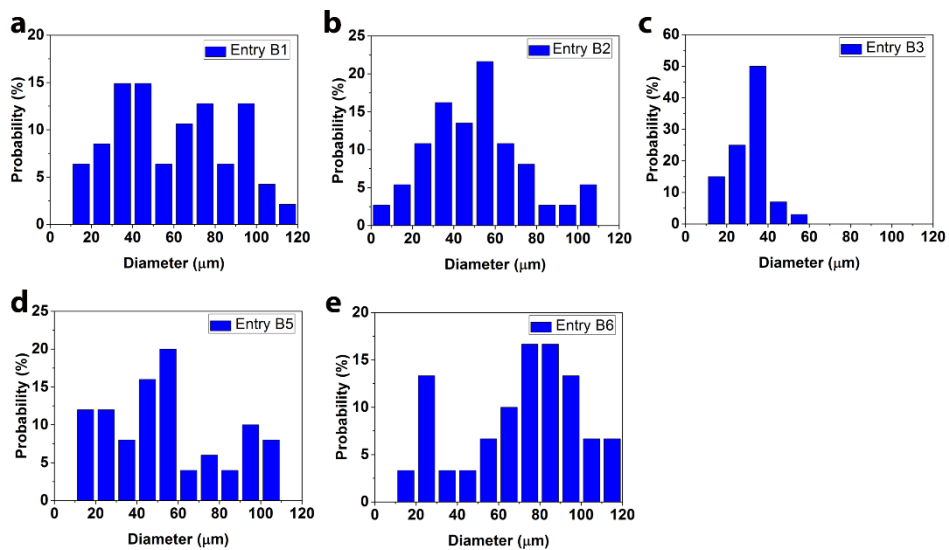


Figure S8. Size distribution of microcapsules from successful microencapsulation in (a) entry B1, (b) entry B2, (c) entry B3, (d) entry B5, and (e) entry B6 listed in Table S4.

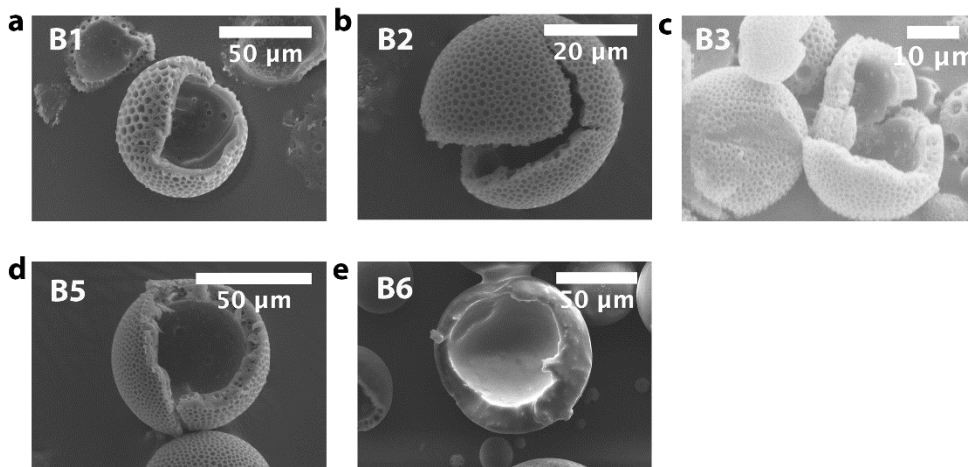


Figure S9. SEM images of crushed cPPA microcapsules showing shell wall thickness in (a) entry B1, (b) entry B2, (c) entry B3, (d) entry B5, and (e) entry B6 listed in Table S4.

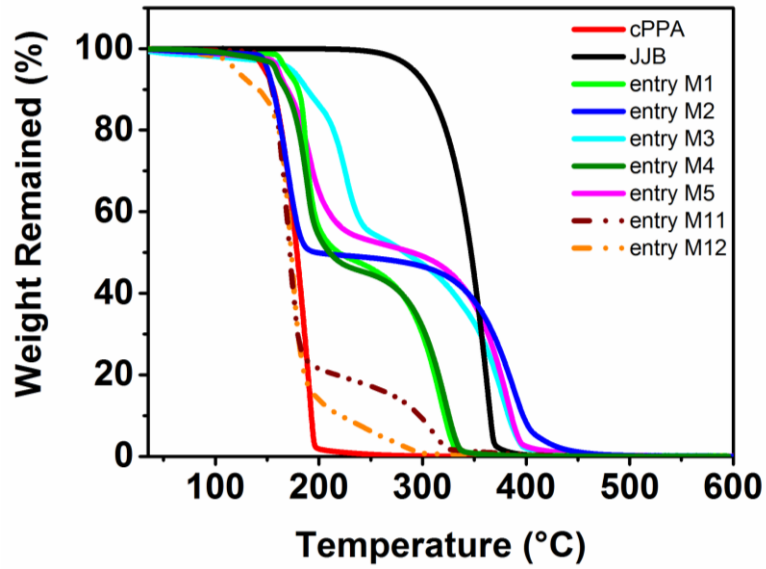


Figure S10. TGA profiles of cPPA microcapsules fabricated from microfluidic emulsification. Preparation ratios were following listed entries M1-M12 in Table S3. TGA profiles of entries M6-M10 in Table S3 were not collected due to low yield.

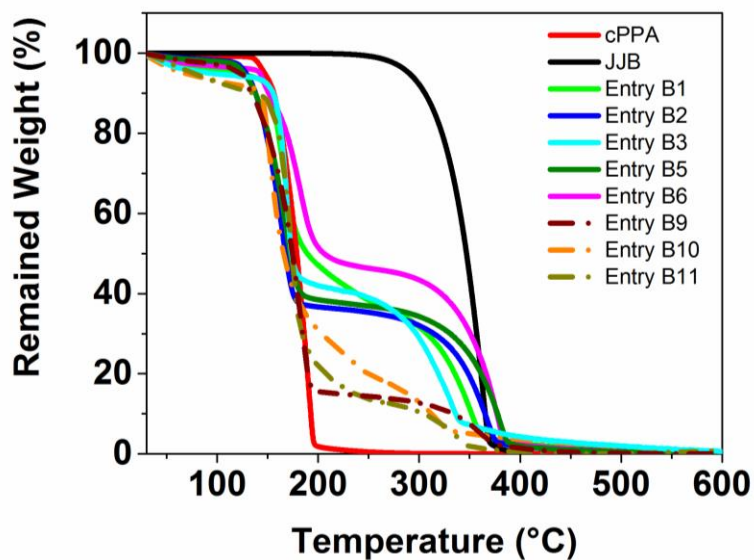


Figure S11. TGA profiles of cPPA microcapsules fabricated from bulk emulsification. Preparation ratios were following listed entries B1-B11 in Table S4. TGA profiles of entries B4, B7 and B8 in Table S4 were not collected due to low yield.

III. Triggered Release Experiments

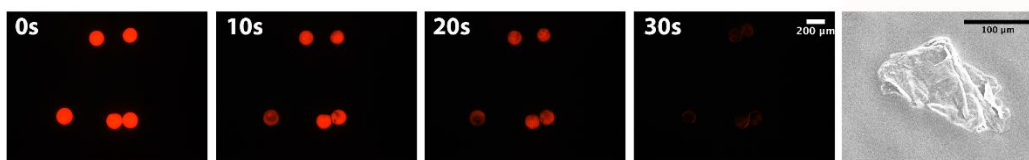


Figure S12. Time sequenced fluorescence microscopy images of cPPA microcapsules in trifluoroacetic acid (TFA) vapor. Image on the right is the SEM image of cPPA microcapsules after exposure in TFA vapor.

IV. Microcapsules Prepared with Different Core Materials and Shell Wall

Table S6. Summary of Encapsulation Parameters

| Entry | Polymer (g) | Core (g) | Solvent (g) | Encapsulation Methods | Evaporation Methods | Morphology |
|-------|------------------------|--------------|----------------------------|--------------------------|------------------------|------------|
| S1 | cPPA 0.1 | DBTL 0.1 | DCM 1.326 | Microfluidics | Vac | Core-shell |
| S2 | cPPA 0.1 | MO 0.1 | DCM 1.326 | Microfluidics | Vac | Core-shell |
| S3 | PV <i>t</i> BCS 0.1 | JJB 0.075 | CHCl ₃ 1.492 | Microfluidics | Vac | Core-shell |

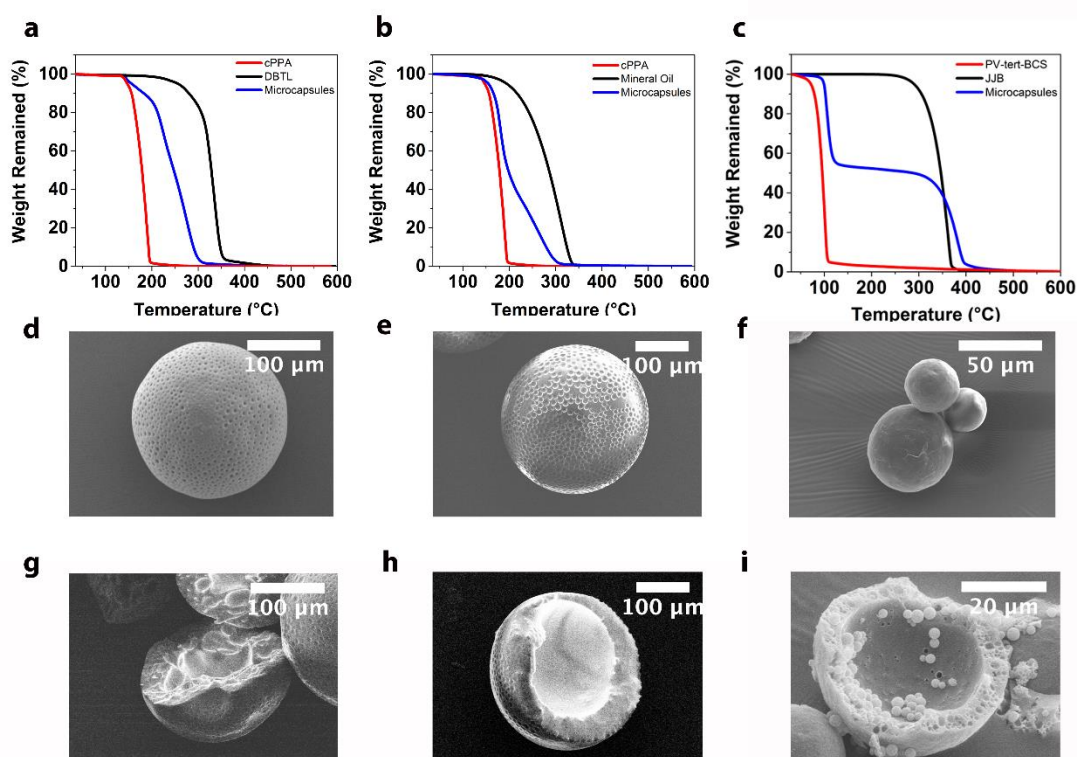


Figure S13. Characterization of cPPA microcapsules with different core materials or different shell wall as listed in Table S6. TGA profiles of (a) cPPA-DBTL microcapsules, (b) cPPA-MO microcapsules and (c) PVtBCS-JJB microcapsules. SEM images of (d) intact cPPA-DBTL microcapsules, (d) intact cPPA-MO microcapsules and (f) PVtBCS-JJB microcapsules; SEM images of broken (g) cPPA-DBTL microcapsules (h) cPPA-MO microcapsules and (i) PVtBCS-JJB microcapsules showing the shell wall thickness and core-shell structure.

1. Kaitz, J. A.; Diesendruck, C. E.; Moore, J. S. End Group Characterization of Poly(phthalaldehyde): Surprising Discovery of a Reversible, Cationic Macrocyclization Mechanism *J. Am. Chem. Soc.* **2013**, *135*, 12755-12761.
2. Lee, O. P.; Lopez Hernandez, H.; Moore, J. S. Tunable Thermal Degradation of Poly(vinyl butyl carbonate sulfone)s via Side-Chain Branching *ACS Macro Lett.* **2015**, *4*, 665-668.